

FedSoL: Bridging Global Alignment and Local Generality in Federated Learning

Gihun Lee¹, Minchan Jeong¹, Sangmook Kim¹, Jaehoon Oh², Se-Young Yun¹,

¹Graduate School of AI, KAIST

²Samsung Advanced Institute of Technology

{opcrisis, mcjeong, sangmook.kim, yunseyoung}@kaist.ac.kr, jh0104.oh@gmail.com

Abstract

Federated Learning (FL) aggregates locally trained models from individual clients to construct a global model. While FL enables learning a model with data privacy, it often suffers from significant performance degradation when client data distributions are heterogeneous. Many previous FL algorithms have addressed this issue by introducing various proximal restrictions. These restrictions aim to encourage global alignment by constraining the deviation of local learning from the global objective. However, they inherently limit local learning by interfering with the original local objectives. Recently, an alternative approach has emerged to improve local learning generality. By obtaining local models within a smooth loss landscape, this approach mitigates conflicts among different local objectives of the clients. Yet, it does not ensure stable global alignment, as local learning does not take the global objective into account. In this study, we propose *Federated Stability on Learning* (FedSoL), which combines both the concepts of global alignment and local generality. In FedSoL, the local learning seeks a parameter region robust against proximal perturbations. This strategy introduces an implicit proximal restriction effect in local learning while maintaining the original local objective for parameter update. Our experiments show that FedSoL consistently achieves state-of-the-art performance on various setups.

1 Introduction

Federated Learning (FL) is an emerging distributed learning framework that preserves data privacy while leveraging client data for training (Konečný et al. 2016b,a). In this approach, individual clients train their local models using their private data, while the server aggregates these models into a global model. By precluding the need for direct access to private data, FL enables the utilization of extensive data collected from edge devices such as mobile phones, vehicles, and facilities (Aledhari et al. 2020; Yang et al. 2019).

However, FL encounters a notorious challenge known as data heterogeneity (Kairouz et al. 2019). Due to the diverse underlying distributions of the clients, the local datasets are non-independent and identically distributed (Non-IID). Its inevitable occurrence in many real-world scenarios leads to an inconsistency between global and local objectives, often significantly degrading performance (Li et al. 2019, 2020a).

To tackle the data heterogeneity problem, most prior studies have introduced various *proximal restriction* into the lo-

cal objective (Karimireddy et al. 2020; Li, He, and Song 2021; Lee et al. 2021; Li et al. 2020b). These restrictions are designed to maintain alignment between global and local objectives by preventing the deviation of local learning from the global objective. Nevertheless, this approach inherently limits local learning by interfering with the original local objectives (Mendieta et al. 2022; Zhang et al. 2022). Furthermore, it often falls into a sharp global landscape under high heterogeneity, which results in unreliable minima and poor stability (Qu et al. 2022; Sun et al. 2023a) (Figure 1(a)).

In contrast, an alternative approach has emerged that focuses on the *local generality* in FL (Qu et al. 2022; Mendieta et al. 2022). Building on recent findings that highlight the benefits of smooth loss landscape for better generalization (Izmailov et al. 2018; Jiang et al. 2019; Chaudhari et al. 2019), this approach aims to seek flatness during local learning by employing the recently proposed Sharpness-Aware Minimization (SAM) (Foret et al. 2020) as the local optimizer (Qu et al. 2022). By improving local generality, this approach mitigates the conflicts between individual local objectives, contributing to the overall smoothness of the aggregated global model (Caldarola, Caputo, and Ciccone 2022; Sun et al. 2023a). Although these approaches have demonstrated competitive performance without the proximal restrictions, their ability to generalize well within their respective local distributions does not necessarily ensure alignment with the global objective (Figure 1(b)).

Our key motivation is to tackle data heterogeneity by harnessing both the strengths of global alignment and local generality. To this end, we propose a novel algorithm Federated Stability on Learning (FedSoL) (Figure 1(c)). FedSoL seamlessly incorporates the proximal restriction effect into the SAM optimization, without interfering with the original local objective. More specifically, FedSoL updates the local model using the gradient of the original local objective, which is determined at the weights perturbed by the gradient of the proximal restriction objective. By identifying a parameter region that is minimally influenced by the proximal perturbation, FedSoL diminishes the negative impact of local updates on global alignment, while maintaining the original local objective to preserve local generality. Furthermore, we control the perturbation strength for each parameter by reflecting the discrepancy between the global and local model parameters. We comprehensively demonstrate the

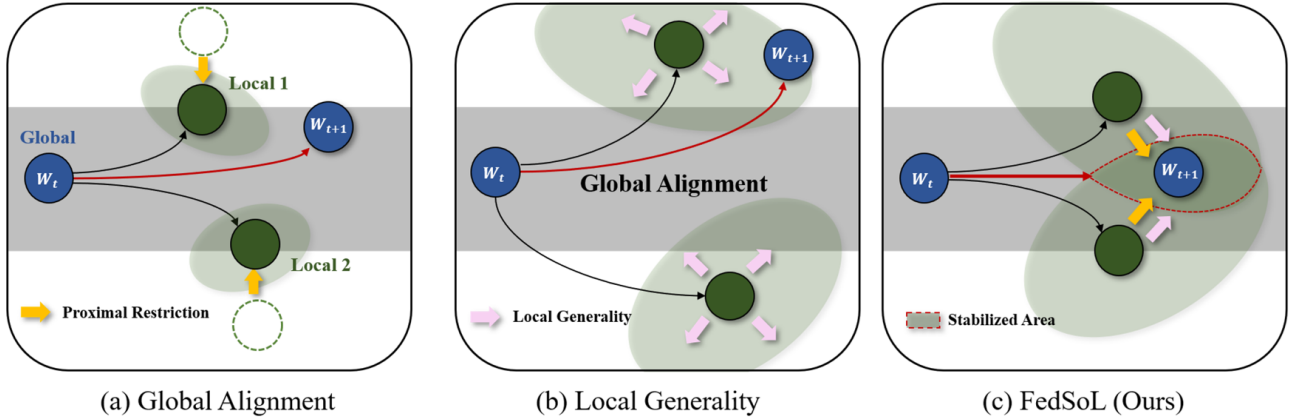


Figure 1: An overview of FL scenarios. Shaded regions stand for the degree of local generality of the trained local models. (a) shows that the local models are aligned with the global objective via proximal restriction, but the local generality is limited. On the other hand, (b) presents enhanced local generality but the local learning deviates from the global objective. In (c), FedSoL integrates the strengths of both scenarios, ensuring global alignment while promoting local generality.

efficacy of FedSoL on global alignment and local generality. Experimental results show FedSoL achieves state-of-the-art performance in various setups. To summarize, our main contributions are as follows:

- We propose FedSoL, a novel and effective FL algorithm that leverages both the strengths of global alignment and local generality. FedSoL conducts proximal perturbations with the SAM strategy, yielding an implicit regularization effect during local learning. (**Section 3**)
- We validate the efficacy of FedSoL on various setups and show that it consistently achieves state-of-the-art performances. We highlight FedSoL performs exceptionally well under high levels of heterogeneity. (**Section 4**)
- We provide a comprehensive analysis of the benefits that FedSoL brings to FL. Not only does it enhance the smoothness of the global model, but it also preserves global knowledge during local learning. (**Section 5**)

2 Background

2.1 Proximal Restriction

Consider an FL system that consists of K clients and a central server. Each client k has a local dataset \mathcal{D}^k , where the entire dataset is a union of the local datasets as $\mathcal{D} = \bigcup_{k \in [K]} \mathcal{D}^k$. FL aims to train a global server model with weights \mathbf{w} that minimize the loss across all clients:

$$\mathcal{L}_{\text{global}}(\mathbf{w}) = \sum_{k \in [K]} \frac{|\mathcal{D}^k|}{|\mathcal{D}|} \mathcal{L}_{\text{local}}^k(\mathbf{w}), \quad (1)$$

where $|\mathcal{D}^k|$ and $|\mathcal{D}|$ are the number of instances in each datasets. When using a proximal restriction objective, the loss function for each client k is a linear combination of its original local loss, $\mathcal{L}_{\text{local}}^k(\mathbf{w}_k)$, and a proximal loss, $\mathcal{L}_p^k(\mathbf{w}_k; \mathbf{w}_g)$, controlled by a hyperparameter β :

$$\mathcal{L}^k(\mathbf{w}_k) = \mathcal{L}_{\text{local}}^k(\mathbf{w}_k) + \beta \cdot \mathcal{L}_p^k(\mathbf{w}_k; \mathbf{w}_g). \quad (2)$$

Here, $\mathcal{L}_{\text{local}}^k(\mathbf{w}_k)$ is the loss on the client’s local distribution (e.g., cross-entropy loss), and $\mathcal{L}_p^k(\mathbf{w}_k; \mathbf{w}_g)$ quantifies the discrepancy between the global model \mathbf{w}_g and the local model \mathbf{w}_k . This discrepancy can be measured in various ways, such as the Euclidean distance between the two parameters (Li et al. 2020b) or the KL-divergence between probability vectors computed using the client’s data (Lee et al. 2021). Introducing proximal restriction within the local objective constrains the deviation of local learning from the global objective (Karimireddy et al. 2020). However, such modified local objective inherently limits the acquisition of new knowledge on the local distribution (Qu et al. 2022).

2.2 Overview of SAM

The SAM (Foret et al. 2020) optimizer pursues flatter minima for the given loss \mathcal{L} by solving the minimax problem:

$$\min_{\mathbf{w}} \max_{\|\epsilon\|_2 < \rho} \mathcal{L}(\mathbf{w} + \epsilon). \quad (3)$$

In the above equation, the inner maximization finds a parameter perturbation ϵ that induces maximal loss change within the ρ -ball neighborhood. In practice, it is approximated by a single re-scaled gradient step $\epsilon^* = \rho \nabla_{\mathbf{w}} \mathcal{L}(\mathbf{w}) / \|\nabla_{\mathbf{w}} \mathcal{L}(\mathbf{w})\|_2$. Then, the outer minimization is conducted by a base optimizer such as SGD (Nesterov 1983), by taking the gradient $\nabla_{\mathbf{w}} \mathcal{L}(\mathbf{w} + \epsilon^*)$ at the perturbed weights. SAM demonstrates an exceptional ability to perform well across different model structures (Chen, Hsieh, and Gong 2021; Zhuang et al. 2022) and tasks (Wang et al. 2023; Abbas et al. 2022) with high generalization performance. In FL, using SAM enhances the generalization of each client’s local model (Qu et al. 2022; Caldarola, Caputo, and Ciccone 2022). However, the deviation of local learning hinders the trained local models to align with each other, preventing the aggregated global model from fully leveraging the advantages of their smoother landscapes (Sun et al. 2023b,a).

3 FedSoL: Federated Stability on Learning

In this section, we introduce Federated Stability on Learning (FedSoL). Our primary motivation is to integrate the proximal restriction effect into the SAM optimization without interfering with the original local objective. The detailed procedure is outlined in Algorithm 1.

3.1 Proximal Perturbation

In local learning, the local model w_k begins with the same parameters as the distributed global model w_g , thereby initially having a minimal proximal loss. The main challenge is guiding the local learning to reduce the original local loss $\mathcal{L}_{\text{local}}^k$ without inducing an increase in the proximal loss \mathcal{L}_p^k . We address this problem in the context of SAM optimization by seeking a gradient that not only minimizes the original local loss $\mathcal{L}_{\text{local}}^k$, but also is robust against the increases in proximal loss \mathcal{L}_p^k . To this end, FedSoL aims to minimize the original local loss, which is minimally affected by the weight perturbation that maximizes proximal loss. By decoupling the roles of these two types of losses, FedSoL conducts the following steps for each local update of client k :

Step1: Weight Perturbation FedSoL finds a weight perturbation ϵ_p^* that causes the most significant change for any given proximal loss \mathcal{L}_p^k :

$$\epsilon_p^* = \rho \frac{\nabla_{w_k} \mathcal{L}_p^k(w_k; w_g)}{\|\nabla_{w_k} \mathcal{L}_p^k(w_k; w_g)\|_2} \approx \operatorname{argmax}_{\|\epsilon\|_2 \leq \rho} \mathcal{L}_p^k(w_k + \epsilon; w_g). \quad (4)$$

Step2: Parameter Update After perturbation, FedSoL updates parameters by computing the gradient of the original local loss $\mathcal{L}_{\text{local}}^k$ at this perturbed weights:

$$w_k \leftarrow w_k - \gamma \cdot \nabla_{w_k} \mathcal{L}_{\text{local}}^k(w_k + \epsilon_p^*), \quad (5)$$

where γ is a learning rate. In the above procedures, the update gradient is computed on the original local loss $\mathcal{L}_{\text{local}}^k$, whereas the proximal loss \mathcal{L}_p^k only plays in an implicit role. Note that ϵ_p^* is used solely for weight perturbation, thereby we do not need to compute its gradient. To clarify how FedSoL influences local learning, we analyze the update gradient g_u of FedSoL by employing the first-order Taylor approximation of $\mathcal{L}_{\text{local}}^k$ at w_k , with perturbation ϵ_p^* :

$$\begin{aligned} g_u(w_k) &= \nabla_{w_k} \mathcal{L}_{\text{local}}^k(w_k + \epsilon_p^*) \\ &\approx g_l(w_k) + \rho \nabla_{w_k}^2 \mathcal{L}_{\text{local}}^k(w_k) \hat{g}_p(w_k). \end{aligned} \quad (6)$$

We denote $g_l = \nabla_{w_k} \mathcal{L}_{\text{local}}^k(w_k)$, $g_p = \nabla_{w_k} \mathcal{L}_p^k(w_k; w_g)$, and $\hat{g}_p = g_p / \|g_p\|_2$, omitting w_k and w_g if there is no conflict. Based on Equation (6), we examine the change of each loss induced by a single local update with a learning rate γ , as defined in Equation (7):

$$\begin{aligned} \Delta^{\text{algo}} \mathcal{L}^k(w_k) &= \mathcal{L}^k(w_k - \gamma g_u(w_k)) - \mathcal{L}^k(w_k) \\ &\approx -\gamma \langle \nabla_{w_k} \mathcal{L}^k(w_k), g_u(w_k) \rangle. \end{aligned} \quad (7)$$

In the above equation, we apply a first-order Taylor approximation to \mathcal{L}^k at w_k , taking into account a local update by $-\gamma g_u(w_k)$. Here, \mathcal{L}^k can be either local loss or proximal loss. By combining the approximation for g_u from Equation (6) into the loss difference in Equation (7), we derive the following two key propositions.

Algorithm 1 Federated Stability on Learning (FedSoL)

Input: local loss $\mathcal{L}_{\text{local}}^k$ and proximal loss \mathcal{L}_p^k for each client $k \in [K]$, learning rate γ , and base perturbation radius ρ

Initialize global server weight w_g

for each communication round t **do**

Server samples clients $K^{(t)} \subset [K]$

Server broadcasts w_g for all $k \in K^{(t)}$

Client replaces $w_k \leftarrow w_g$

for each client $k \in K^{(t)}$ **in parallel do**

for each local step **do**

Set Adaptive Perturbation Radius (Sec 3.2)

$\rho_{\text{adaptive}} = \rho \cdot \Lambda$ (element-wise rescale)

Perturb using Proximal Gradient (Sec 3.1)

$\epsilon_p^* = \rho_{\text{adaptive}} \odot \frac{\nabla_{w_k} \mathcal{L}_p^k(w_k; w_g)}{\|\nabla_{w_k} \mathcal{L}_p^k(w_k; w_g)\|}$

Update Local Model Parameters (Sec 3.1)

$w_k \leftarrow w_k - \gamma \cdot \nabla_{w_k} \mathcal{L}_{\text{local}}^k(w_k + \epsilon_p^*)$

end for

end for

Upload w_k to server

Server Aggregation : $w_g \leftarrow \frac{1}{|K^{(t)}|} \sum_{k \in K^{(t)}} w_k$

end for

Server output : w_g

Proposition 1 Given a convex local loss $\mathcal{L}_{\text{local}}^k$, the change of proximal loss \mathcal{L}_p^k by FedSoL update with a learning rate γ reduces the conflicts between g_l and g_p as ρ grows:

$$\Delta^{\text{FedSoL}} \mathcal{L}_p^k \approx -\gamma \left(\langle g_l, g_p \rangle + \underbrace{\rho \cdot \hat{g}_p^\top \nabla^2 \mathcal{L}_{\text{local}}^k g_p}_{\geq 0} \right), \quad (8)$$

where $\nabla^2 \mathcal{L}_{\text{local}}^k$ is the Hessian at w_k . In **Proposition 1**, we study the change of proximal loss after the FedSoL update, denoted as $\Delta^{\text{FedSoL}} \mathcal{L}_p^k$. The proposition suggests that FedSoL implicitly regularizes local learning for global alignment, reducing the negative impact of local updates on proximal loss. This regularization effect grows as the curvature of local loss $\nabla^2 \mathcal{L}_{\text{local}}^k$ becomes steeper. Note that when ρ is set to 0, Equation (8) becomes the change of proximal loss after FedAvg update, $\Delta^{\text{FedAvg}} \mathcal{L}_p^k$.

Proposition 2 The change of original local loss $\mathcal{L}_{\text{local}}^k$ by FedSoL update with a learning rate γ is equivalent to the FedAvg update at $\nabla \mathcal{L}_{\text{local}}^k(w_k + \frac{\rho}{2} \epsilon_p^*)$ as:

$$\Delta^{\text{FedSoL}} \mathcal{L}_{\text{local}}^k(w_k) \approx \Delta^{\text{FedAvg}} \mathcal{L}_{\text{local}}^k \left(w_k + \frac{\rho}{2} \epsilon_p^* \right). \quad (9)$$

Meanwhile, **Proposition 2** analyzes how the original local loss changes after the FedSoL update, $\Delta^{\text{FedSoL}} \mathcal{L}_{\text{local}}^k$, and compare it to its counterpart in FedAvg, $\Delta^{\text{FedAvg}} \mathcal{L}_{\text{local}}^k$. The proposition suggests that even though FedSoL calculates the gradient of the original local loss at the weight perturbed by proximal gradient, its behavior on the original local loss is almost identical to that of FedAvg with standard gradient descent using $\mathcal{L}_{\text{local}}^k$. This implies that FedSoL does not noticeably interfere with or slow down the learning process on the local data distribution. The detailed proofs for the propositions are provided in Appendix.

3.2 Adaptive Perturbation Radius

While SAM defines a fixed radius ρ , it is often insufficient in capturing the loss landscape dynamics (Kwon et al. 2021; Kim et al. 2022). In FedSoL, we introduce an adaptive radius reflecting the global and local parameter discrepancies. For each layer m , we construct a scaling vector $\lambda^{(m)}$, where the i -th entry corresponds to each parameter in that layer:

$$\lambda^{(m)}[i] = \frac{|\mathbf{w}_k^{(m)}[i] - \mathbf{w}_g^{(m)}[i]|}{\|\mathbf{w}_k^{(m)} - \mathbf{w}_g^{(m)}\|_2}. \quad (10)$$

Here, $\mathbf{w}_g^{(m)}$ and $\mathbf{w}_k^{(m)}$ denote layer m in the global and local model respectively. The denominator represents the normalization of the discrepancy within the layer, accounting for the layer-wise scale variance. The adaptive radius allows more perturbation for the parameter with large difference, and vice versa. It fits with the typical behavior of proximal loss, which increases as $\|\mathbf{w}_k - \mathbf{w}_g\|_2$ grows. By concatenating these layer-specific vectors, $\Lambda = (\lambda^{(1)}, \dots, \lambda^{(m)}, \dots, \lambda^{(\text{last})})$, and incorporating it into the Equation (4), the proximal perturbation ϵ_p^* becomes:

$$\begin{aligned} \epsilon_p^* &= \rho \cdot \Lambda \odot \frac{\nabla_{\mathbf{w}_k} \mathcal{L}_p^k(\mathbf{w}_k; \mathbf{w}_g)}{\|\nabla_{\mathbf{w}_k} \mathcal{L}_p^k(\mathbf{w}_k; \mathbf{w}_g)\|_2} \\ &\approx \underset{\|\Lambda^{-1} \odot \epsilon\|_2 \leq \rho}{\text{argmax}} \mathcal{L}_p^k(\mathbf{w}_k + \epsilon; \mathbf{w}_g), \end{aligned} \quad (11)$$

where \odot denotes the element-wise product. Intuitively, the adaptive radius allows local learning to deviate certain parameters from the global model, only if they are crucial enough to withstand larger weight perturbations.

4 Experiment

4.1 Experimental Setups

Data Setups We employ 6 datasets: MNIST (Deng 2012), CIFAR-10 (Krizhevsky, Nair, and Hinton 2009), SVHN (Netzer et al. 2011), CINIC-10 (Darlow et al. 2018), PathMNIST (Yang et al. 2023), and TissueMNIST (Yang et al. 2023). We distribute data to clients via two strategies: Sharding (McMahan et al. 2017) and Latent Dirichlet Allocation (LDA) (Wang et al. 2020a). Sharding sorts data by label and assigns equal-size shards to clients. The heterogeneity increases as the shard per user, s , becomes smaller. On the other hand, LDA assigns class c data samples to each client k with probability $p_c (\approx \text{Dir}(\alpha))$, where the heterogeneity increases as α , becomes smaller. Figure 2 illustrates the difference between these partition strategies.

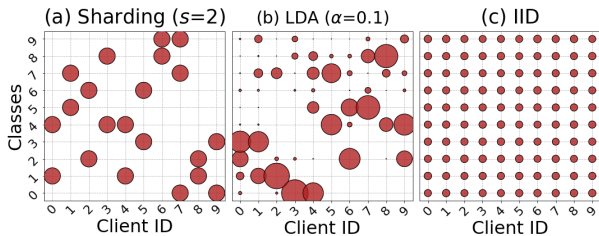


Figure 2: CIFAR-10 partition examples across 10 clients.

Learning Setups We distribute MNIST, CIFAR-10, and SVHN datasets across 100 clients with a sampling ratio of 0.1, while CINIC-10, PathMNIST, and TissueMNIST across 200 clients with a ratio of 0.05. We use a model architecture as described in (McMahan et al. 2017), which consists of two convolutional layers, max-pooling layers, and two fully connected layers. Each client optimizes its local datasets for 5 local epochs using momentum SGD with a learning rate of 0.01, momentum 0.9, and weight decay $1e-5$. The learning rate is decayed by a factor of 0.99 at every communication round. We conduct 300 communication rounds in general, and 200 for MNIST, PathMNIST, and TissueMNIST, which is enough for the server model’s performance to reach saturation. We use KL-divergence loss as the proximal loss.

4.2 Effect on Local Learning

Proximal Restriction We examine the proximal restriction effect in FedSoL by analyzing how its update gradient g_u interacts with the proximal loss \mathcal{L}_p , as shown in Figure 3. As ρ increases, g_u becomes more orthogonal to the proximal gradient g_p (Figure 3(b)). This orthogonality helps in maintaining the proximal loss low during the local learning process, which implies better global alignment (Figure 3(a)).

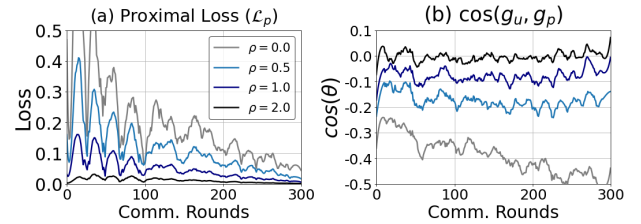


Figure 3: Effect of FedSoL on local learning in CIFAR-10 ($\alpha=0.1$) by varying ρ values. (a) Average proximal loss of local models. (b) Cosine similarity between FedSoL gradient (g_u) and proximal gradient (g_p) during local learning.

Adaptive Radius The advantage of the adaptive approach are depicted in Figure 4. As shown in Figure 4(a), using the adaptive radius not only improve performance but also reduces sensitivity to the selection of ρ . Meanwhile, Figure 4(b) displays the averaged λ values for each local model layer, highlighting the increased deviation in the later layers, as a consequence of the data heterogeneity (Luo et al. 2021). Note that using a fixed value for ρ corresponds to setting Λ in Equation (11) as a vector with all entries to one.

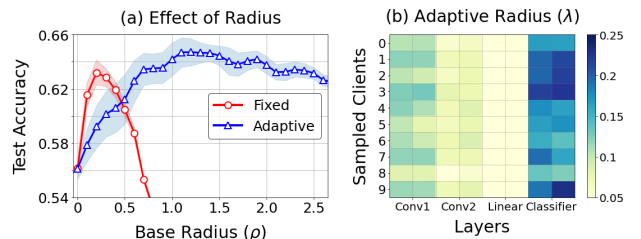


Figure 4: Effect of adaptive radius in CIFAR-10 ($\alpha=0.1$). (a) Server test accuracy after 300 rounds. (b) Layer-wisely averaged λ values of FedSoL ($\rho = 1.0$) at round 200.

Table 1: Test accuracy@1(%) comparison among baselines and FedSoL on different datasets. The values in the parenthesis are the standard deviation. The arrow (\downarrow , \uparrow) shows the comparison to the FedAvg. We set $s \in \{2, 3, 5, 10\}$ and $\alpha \in \{0.05, 0.1, 0.3, 0.5\}$ for CIFAR-10 datasets, whereas $s = 2$ and $\alpha = 0.1$ for the others.

Non-IID Partition Strategy : Sharding									
Method	MNIST	CIFAR-10				SVHN	CINIC-10	PathMNIST	TissueMNIST
		$s = 2$	$s = 3$	$s = 5$	$s = 10$				
FedAvg	96.16 _(0.19)	51.48 _(3.41)	62.94 _(0.00)	70.96 _(0.91)	74.60 _(0.88)	73.63 _(3.16)	42.40 _(2.70)	57.40 _(1.48)	49.36 _(1.64)
FedProx	95.86 _(0.12)	\downarrow 52.80 _(2.66)	\uparrow 58.19 _(0.55)	\downarrow 64.71 _(0.74)	\downarrow 69.37 _(1.21)	\downarrow 71.09 _(3.13)	\downarrow 40.00 _(3.01)	\downarrow 60.77 _(3.64)	\uparrow 48.20 _(1.95)
FedNova	94.13 _(0.36)	\downarrow 46.89 _(2.57)	\downarrow 61.12 _(0.88)	\downarrow 67.11 _(0.25)	\downarrow 70.59 _(0.52)	\downarrow 67.35 _(2.84)	\downarrow 40.94 _(2.29)	\downarrow 58.85 _(4.10)	\uparrow 36.44 _(0.95)
Scaffold	95.91 _(0.18)	\downarrow 62.60 _(0.70)	\uparrow 68.53 _(0.99)	\uparrow 74.28 _(0.39)	\uparrow 76.71 _(0.16)	\uparrow 77.84 _(2.28)	\uparrow 47.76 _(0.45)	\uparrow 71.12 _(1.04)	\downarrow 30.99 _(6.09)
FedNTD	96.62 _(0.06)	\uparrow 67.25 _(1.08)	\uparrow 70.47 _(0.33)	\uparrow 75.21 _(0.39)	\uparrow 76.46 _(0.07)	\uparrow 85.30 _(0.78)	\uparrow 52.72 _(1.12)	\uparrow 65.00 _(1.26)	\uparrow 52.63 _(0.59)
FedSAM	96.12 _(0.19)	\uparrow 51.85 _(3.14)	\uparrow 60.90 _(0.93)	\downarrow 69.29 _(0.39)	\downarrow 72.98 _(0.34)	\downarrow 65.85 _(3.77)	\downarrow 45.91 _(2.02)	\uparrow 67.32 _(3.15)	\uparrow 49.62 _(1.61)
FedASAM	97.08 _(0.15)	\uparrow 52.08 _(2.19)	\uparrow 63.24 _(1.16)	\uparrow 70.95 _(0.76)	\downarrow 74.74 _(0.88)	\uparrow 79.48 _(2.17)	\downarrow 43.15 _(2.73)	\uparrow 59.47 _(2.91)	\uparrow 49.46 _(1.91)
FedSoL (Ours)	97.15 _(0.08)	\uparrow 66.72 _(0.61)	\uparrow 69.88 _(0.15)	\uparrow 75.82 _(0.34)	\uparrow 77.79 _(0.19)	\uparrow 85.18 _(0.37)	\uparrow 55.17 _(0.32)	\uparrow 73.85 _(1.55)	\uparrow 53.42 _(0.46)

Non-IID Partition Strategy : LDA									
Method	MNIST	CIFAR-10				SVHN	CINIC-10	PathMNIST	TissueMNIST
		$\alpha = 0.05$	$\alpha = 0.1$	$\alpha = 0.3$	$\alpha = 0.5$				
FedAvg	96.11 _(0.19)	42.27 _(1.34)	56.13 _(0.78)	67.32 _(0.94)	73.90 _(0.66)	55.36 _(4.85)	36.49 _(4.37)	65.98 _(4.76)	42.78 _(2.03)
FedProx	96.05 _(0.13)	\downarrow 50.58 _(0.57)	\uparrow 59.80 _(1.12)	\uparrow 68.39 _(0.81)	\uparrow 72.87 _(0.55)	\uparrow 72.40 _(3.15)	\uparrow 40.09 _(3.97)	\uparrow 70.44 _(1.92)	\uparrow 52.25 _(1.40)
FedNova	88.24 _(1.37)	\downarrow 10.00 _(Failed)	\downarrow 10.00 _(Failed)	\downarrow 64.67 _(0.77)	\downarrow 70.04 _(0.45)	\downarrow 53.07 _(3.30)	\downarrow 21.89 _(1.71)	\downarrow 38.94 _(2.34)	\downarrow 15.03 _(3.74)
Scaffold	94.18 _(0.32)	\downarrow 10.00 _(Failed)	\downarrow 10.00 _(Failed)	\downarrow 71.92 _(0.17)	\downarrow 75.49 _(0.21)	\downarrow 21.46 _(1.75)	\downarrow 16.89 _(2.25)	\downarrow 18.07 _(0.04)	\downarrow 32.04 _(0.07)
FedNTD	96.97 _(0.27)	\uparrow 58.08 _(0.48)	\uparrow 63.16 _(1.02)	\uparrow 71.56 _(0.26)	\uparrow 74.91 _(0.33)	\uparrow 79.25 _(0.61)	\uparrow 50.22 _(3.71)	\uparrow 74.26 _(1.25)	\uparrow 44.55 _(1.95)
FedSAM	95.72 _(0.43)	\downarrow 36.14 _(1.21)	\downarrow 52.14 _(0.94)	\downarrow 64.83 _(0.56)	\downarrow 70.74 _(0.40)	\downarrow 13.27 _(2.78)	\downarrow 36.70 _(4.28)	\uparrow 66.64 _(3.76)	\uparrow 44.07 _(3.02)
FedASAM	96.60 _(0.10)	\uparrow 43.12 _(1.25)	\uparrow 57.00 _(0.30)	\uparrow 67.45 _(0.92)	\uparrow 73.91 _(0.51)	\uparrow 60.25 _(4.56)	\uparrow 36.93 _(4.60)	\uparrow 69.45 _(3.19)	\uparrow 42.73 _(2.35)
FedSoL (Ours)	97.44 _(0.11)	\uparrow 60.01 _(0.30)	\uparrow 64.13 _(0.46)	\uparrow 71.94 _(0.57)	\uparrow 75.60 _(0.32)	\uparrow 83.92 _(0.29)	\uparrow 55.07 _(1.48)	\uparrow 78.88 _(0.46)	\uparrow 53.40 _(0.85)

4.3 Performance on Data Heterogeneity

Heterogeneity Level Table 1 presents a comparison between our approach, FedSoL, and other baselines such as FedProx (Li et al. 2020b), FedNova (Wang et al. 2020b), Scaffold (Karimireddy et al. 2020), FedNTD (Lee et al. 2021), FedSAM (Qu et al. 2022), and FedASAM (Caldarola, Caputo, and Ciccone 2022) as baseline methods. Notably, many recently proposed FL methods tend to underperform when compared to the standard FedAvg baseline, where a similar observation is reported in (Zhao et al. 2018; Lee et al. 2021). In contrast, FedSoL consistently exceeds the performance of FedAvg across all evaluated scenarios. FedSoL achieves state-of-the-art results in most cases, particularly showing consistent improvement on high heterogeneity levels ($s=2$ and $\alpha=0.05$).

Learning Factors In Figure 5, we examine the learning factors that influence FedSoL’s performance: Partial Participation (Figure 5(a)), Number of Local Epochs (Figure 5(b)), and Learning Rate (Figure 5(c)). Throughout experiments, FedSoL consistently surpasses the FedAvg across varying factors. Most of all, FedSoL enlarges its gain as the smaller portion of clients participate in each round. For instance, FedAvg significantly declines in performance at a sampling ratio of 0.02, reaching to a near-random accuracy. However, FedSoL maintains robust performance under such condition.

Perturbation Strength In FedSoL, a hyperparameter ρ controls the overall perturbation strength. Figure 5(d) plots FedSoL’s performance against varying ρ values. Although

the model often diverges when using the SAM strategy with high perturbation strength (as shown in Table 1), our FedSoL remains relatively robust and achieve its best performance within the ρ range between 0.5 and 2.0.

Model Architecture We conduct further experiments on different model architectures: VggNet-11 (Simonyan and Zisserman 2014), ResNet-18 (He et al. 2016), and SL-ViT (Lee, Lee, and Song 2021), which is a specialized structure of ViT (Dosovitskiy et al. 2020) for small-sized datasets. The results provided in Table 2 validates the efficiency of FedSoL across varying model architectures.

Table 2: Comparison of method on different model architectures. The heterogeneity is set as LDA ($\alpha = 0.1$).

Model	Method	CIFAR-10	SVNH	PathMNIST
Vgg11	FedAvg	41.30 \pm 1.07	50.02 \pm 4.25	61.79 \pm 9.88
	FedProx	40.45 \pm 1.41	31.07 \pm 6.72	63.47 \pm 2.68
	FedNTD	60.55 \pm 2.14	56.62 \pm 2.64	69.82 \pm 2.27
	FedSoL	56.39 \pm 1.40	74.74 \pm 0.04	78.38 \pm 1.12
Res18	FedAvg	49.92 \pm 0.62	76.98 \pm 2.90	57.91 \pm 1.27
	FedProx	59.00 \pm 2.58	82.09 \pm 2.35	75.84 \pm 1.58
	FedNTD	57.79 \pm 3.42	78.50 \pm 0.18	76.87 \pm 0.57
	FedSoL	66.32 \pm 0.48	85.97 \pm 0.04	80.59 \pm 0.11
SL-ViT	FedAvg	35.48 \pm 2.09	53.94 \pm 5.17	72.44 \pm 1.91
	FedProx	38.73 \pm 1.23	58.25 \pm 4.23	74.10 \pm 1.23
	FedNTD	47.59 \pm 2.84	61.46 \pm 1.76	71.65 \pm 1.71
	FedSoL	47.95 \pm 1.51	67.19 \pm 0.33	77.96 \pm 0.47

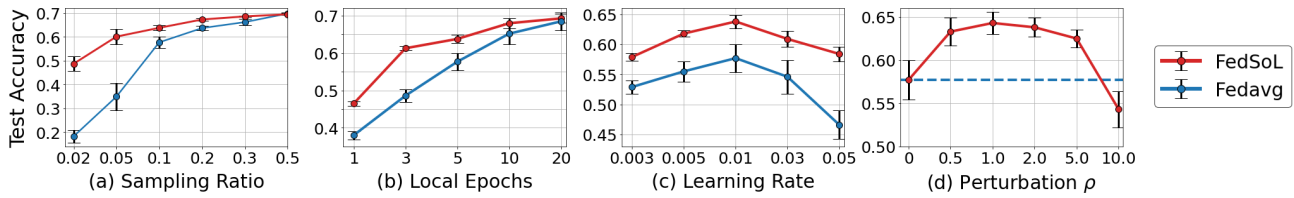


Figure 5: Performance of *FedAvg* and *FedSoL* on CIFAR-10 ($\alpha=0.1$) with various setups: (a) sampling ratio, (b) the number of local epochs, (c) initial learning rate, and (d) perturbation strength. The error bars stand for the standard deviations.

4.4 Proximal Losses

In our primary experiments, we utilize KL-divergence loss as the proximal loss. However, FedSoL can be combined with various other proximal objectives. Table 3 shows the impact of incorporating FedSoL with other proximal restrictions: FedProx (Li et al. 2020b), FedNova (Wang et al. 2020b), Scaffold (Karimireddy et al. 2020), FedDyn (Acar et al. 2021), and Moon (Li, He, and Song 2021). These methods are compared in two distinct scenarios: as an auxiliary objective alongside the original local objective (Base) and as proximal perturbation within FedSoL (Combined). The results show the enhanced performances with FedSoL.

Table 3: Comparison of proximal methods combined with FedSoL ($\rho=2.0$). The heterogeneity is set as LDA ($\alpha = 0.1$).

Method	CIFAR-10		SVHN		CINIC-10	
	Base	Combined	Base	Combined	Base	Combined
FedProx	59.80	63.93 ↑	72.40	84.32 ↑	40.09	55.25 ↑
FedNova	10.00	31.77 ↑	53.07	79.95 ↑	21.89	42.37 ↑
Scaffold	10.00	62.70 ↑	21.46	77.52 ↑	16.89	49.96 ↑
FedDyn	60.80	62.85 ↑	78.15	79.43 ↑	48.25	52.17 ↑
MOON	55.72	60.91 ↑	29.67	76.82 ↑	38.15	49.14 ↑

4.5 Partial Perturbation

As the data heterogeneity does not affect all layers equally (Luo et al. 2021), we investigate the use of *partial* perturbation in FedSoL, by selectively perturbing specific layers instead of the entire model. The results in Table 4 reveal that perturbing only the last classifier layer (*Head* in Table 4) is sufficient for FedSoL. The performance is nearly as high as the full-model perturbation, but the computational requirement is significantly lower by avoiding multiple forward and backward computations across all layers when using the standard SAM strategy. Interestingly, perturbing all layers except the classifier head (*Body* in Table 4) consumes almost the same amount of computation but rather drops in performance, showing the importance of the later layers.

Table 4: Effect of partial weight perturbation in CIFAR10 ($\alpha=0.1$). The FLOPs shows relative computation w.r.t. FedAvg. δ stands for the computation for the proximal loss.

Target Position	Perturbation (ρ)					FLOPs
	0.0	0.5	1.0	1.5	2.0	
All (<i>full</i>)		61.17	64.16	64.38	63.94	$2\times +\delta$
Body (<i>partial</i>)	56.13	60.98	62.95	63.94	63.80	$1.96\times +\delta$
Head (<i>partial</i>)		62.65	63.62	64.13	63.25	$1.33\times +\delta$

5 Analysis

In this section, we explore how FedSoL benefits in FL. We demonstrate that FedSoL not only smooths the loss landscape of the learned model but also ensures that local learning stays closely aligned with the global model. This alignment retains the knowledge of the global distribution.

5.1 Weight Divergence

To assess the deviation of local learning from the global model, we measure the L2 distance between models: $\|w_g - w_k\|$ where w_g is the global model and w_k is the client k 's trained local model. The results, averaged across sampled clients, are shown in Figure 6. In Figure 6(a), FedSoL effectively reduces the divergence, ensuring that local models remain closely aligned with the global model, verifying the proximal restriction effect in FedSoL. Figure 6(b) illustrates that this alignment also fosters increased consistency among local models, reducing their mutual divergence.

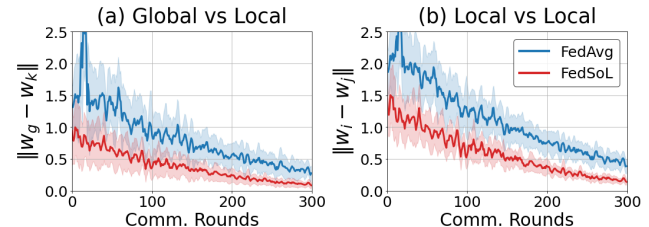


Figure 6: Comparative analysis of weight divergence in FedAvg and FedSoL ($\rho=2.0$) on CIFAR-10 LDA ($\alpha=0.1$). (a) shows global-local model divergence, while (b) presents the divergence across local models.

5.2 Knowledge Preservation

To understand how FedSoL stabilizes the local learning at the prediction level, we examine how well a local model maintains its performance on the global distribution after local learning. As illustrated in Figure 7(a), FedAvg's local models undergo a significant drop in performance on the global distribution after local learning. Conversely, FedSoL maintains high performance, indicating better alignment of local learning with the global objective, and thus stabilizing the learning process. We further analyze the class-wise accuracy of FedAvg and FedSoL server models. As Figure 7(b) demonstrates, while FedAvg exhibits significant fluctuations and inconsistent class-wise performance, FedSoL preserves its class-wise accuracy as the communication proceeds.

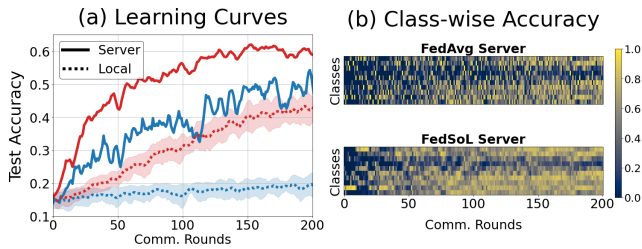


Figure 7: Comparison of FedAvg (blue lines) and FedSoL ($\rho=2.0$) (red lines) on CIFAR-10 ($s=2$). (a) shows learning curves for global and local models, with shaded areas reflecting standard deviation across clients. (b) exhibits the class-wise accuracy of the global model.

5.3 Smoothness of Loss Landscape

We visualize the loss landscapes (Li et al. 2018) of global models obtained from FedAvg, FedASAM, and FedSoL in Figure 8. In these plots, each axis corresponds to one of the two dominant eigenvectors (top-1 and top-2) of the Hessian matrix, representing the directions of the most significant shifts in the loss landscape. Along with each landscape, we provide the value of the dominant eigenvalue (λ_1) and its ratio to the fifth largest eigenvalue (λ_1/λ_5), following the criteria used in (Foret et al. 2020; Mi et al. 2022). Here, FedSoL’s smaller ratio indicates that the variations in loss are more evenly distributed across various directions. Both the landscape visualization and Hessian eigenvalues underscore the efficacy of FedSoL in smoothing the loss landscape.

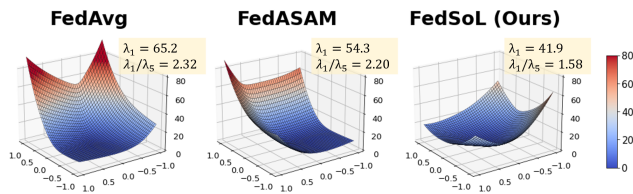


Figure 8: Loss landscape visualization of global model on CIFAR-10 LDA ($\alpha=0.1$). The λ_1 and λ_5 in each figure stand for the top-1 and top-5 eigenvalues of the Hessian matrix.

6 Related Work

6.1 Federated Learning (FL)

Federated learning is a distributed learning paradigm to train models without directly accessing private client data (Konečný et al. 2016b,a). The standard algorithm, FedAvg (McMahan et al. 2017), aggregates locally trained models by averaging their parameters. While a variety of FL algorithms have been introduced, they commonly conduct parameter averaging in a certain manner (Li et al. 2020b; Karimireddy et al. 2020; Lee et al. 2021; Zhang et al. 2022). Although FedAvg ideally performs well when all client devices are active and IID distributed (Stich 2018; Woodworth et al. 2020), its performance significantly degrades when clients have heterogeneous data distributions (Zhao et al. 2018; Li et al. 2019; Kairouz et al. 2019). Our work focuses

on mitigating this data heterogeneity issue by modifying the local learning strategy.

6.2 Proximal Restriction in FL

A prevalent strategy to address data heterogeneity in FL is the introduction of a proximal term into local learning objectives (Lee et al. 2021; Li et al. 2020b; Karimireddy et al. 2020; Li, He, and Song 2021). This approach aims to restrict the local learning deviation induced by the biased local distributions. For example, FedProx (Li et al. 2020b) employs L_2 distance between models, while MOON (Li, He, and Song 2021) uses the contrastive loss (Oord, Li, and Vinyals 2018), regarding the previously trained local model’s representations as negative pairs. Meanwhile, Scaffold (Karimireddy et al. 2020) use estimated global direction as a control variate to adjust local gradients. However, such explicit alteration of local objectives may hinder the acquisition of new knowledge during local learning (Qu et al. 2022; Mendieta et al. 2022). In our study, we aim to leverage the benefits of proximal restriction effect during local learning, but without changing the original local objectives.

6.3 SAM Optimization in FL

Recent studies have begun to suggest that enhancing local learning generality can significantly boost FL performance (Mendieta et al. 2022; Qu et al. 2022; Caldarola, Caputo, and Ciccone 2022), aiding the global model in generalizing more effectively. Inspired by the latest findings that connect loss geometry to the generalization gap (Izmailov et al. 2018; Keskar et al. 2016; Jiang et al. 2019; Chaudhari et al. 2019), those works seek for *flat minima*, utilizing the recently proposed Sharpness-Aware Minimization (SAM) (Foret et al. 2020) as the local optimizer. For instance, FedSAM (Qu et al. 2022) and FedASAM (Caldarola, Caputo, and Ciccone 2022) demonstrate the benefits of using SAM and its variants as local optimizer. Meanwhile, FedSMO (Sun et al. 2023a) incorporates a global-level SAM optimizer, and FedSpeed (Sun et al. 2023b) employs multiple gradient calculations to encourage global consistency. In our work, we introduce the proximal restriction effect into SAM in an implicit manner, by adjusting the perturbation direction and magnitude during local learning.

7 Conclusion

We believe that FL serves as a crucial learning paradigm that opens up extensive data utilization under the growing concerns on data privacy. In this study, we emphasize the importance of both global alignment and local generality in tackling data heterogeneity within FL. To unify these essential components, we propose Federated Stability on Learning (FedSoL), a novel and versatile method that seeks a robust parameter region against proximal weight perturbations. This allows for an implicit proximal restriction effect on local learning, without interfering with the original local objective. We present a comprehensive analysis of FedSoL and demonstrate its benefits in FL. The insights provided in our work may inspire new research directions, furthering our understanding of FL and its potential applications.

References

- Abbas, M.; Xiao, Q.; Chen, L.; Chen, P.-Y.; and Chen, T. 2022. Sharp-maml: Sharpness-aware model-agnostic meta learning. In *International conference on machine learning*, 10–32. PMLR.
- Acar, D. A. E.; Zhao, Y.; Navarro, R. M.; Mattina, M.; Whatmough, P. N.; and Saligrama, V. 2021. Federated learning based on dynamic regularization. *arXiv preprint arXiv:2111.04263*.
- Aledhari, M.; Razzak, R.; Parizi, R. M.; and Saeed, F. 2020. Federated learning: A survey on enabling technologies, protocols, and applications. *IEEE Access*, 8: 140699–140725.
- Caldarola, D.; Caputo, B.; and Ciccone, M. 2022. Improving Generalization in Federated Learning by Seeking Flat Minima. *arXiv preprint arXiv:2203.11834*.
- Chaudhari, P.; Choromanska, A.; Soatto, S.; LeCun, Y.; Baldassi, C.; Borgs, C.; Chayes, J.; Sagun, L.; and Zecchina, R. 2019. Entropy-sgd: Biasing gradient descent into wide valleys. *Journal of Statistical Mechanics: Theory and Experiment*, 2019(12): 124018.
- Chen, X.; Hsieh, C.-J.; and Gong, B. 2021. When vision transformers outperform resnets without pre-training or strong data augmentations. *arXiv preprint arXiv:2106.01548*.
- Darlow, L. N.; Crowley, E. J.; Antoniou, A.; and Storkey, A. J. 2018. Cinic-10 is not imagenet or cifar-10. *arXiv preprint arXiv:1810.03505*.
- Deng, J.; Dong, W.; Socher, R.; Li, L.-J.; Li, K.; and Fei-Fei, L. 2009. Imagenet: A large-scale hierarchical image database. In *2009 IEEE conference on computer vision and pattern recognition*, 248–255. Ieee.
- Deng, L. 2012. The mnist database of handwritten digit images for machine learning research. *IEEE Signal Processing Magazine*, 29(6): 141–142.
- DeVries, T.; and Taylor, G. W. 2017. Improved regularization of convolutional neural networks with cutout. *arXiv preprint arXiv:1708.04552*.
- Dosovitskiy, A.; Beyer, L.; Kolesnikov, A.; Weissenborn, D.; Zhai, X.; Unterthiner, T.; Dehghani, M.; Minderer, M.; Heigold, G.; Gelly, S.; et al. 2020. An image is worth 16x16 words: Transformers for image recognition at scale. *arXiv preprint arXiv:2010.11929*.
- Fallah, A.; Mokhtari, A.; and Ozdaglar, A. 2020. Personalized federated learning with theoretical guarantees: A model-agnostic meta-learning approach. *Advances in Neural Information Processing Systems*, 33: 3557–3568.
- Foret, P.; Kleiner, A.; Mobahi, H.; and Neyshabur, B. 2020. Sharpness-aware minimization for efficiently improving generalization. *arXiv preprint arXiv:2010.01412*.
- He, C.; Li, S.; So, J.; Zeng, X.; Zhang, M.; Wang, H.; Wang, X.; Vepakomma, P.; Singh, A.; Qiu, H.; et al. 2020. Fedml: A research library and benchmark for federated machine learning. *arXiv preprint arXiv:2007.13518*.
- He, K.; Zhang, X.; Ren, S.; and Sun, J. 2016. Identity mappings in deep residual networks. In *European conference on computer vision*, 630–645. Springer.
- Hinton, G.; Vinyals, O.; and Dean, J. 2015. Distilling the knowledge in a neural network. *arXiv preprint arXiv:1503.02531*.
- Izmailov, P.; Podoprikin, D.; Garipov, T.; Vetrov, D.; and Wilson, A. G. 2018. Averaging weights leads to wider optima and better generalization. *arXiv preprint arXiv:1803.05407*.
- Jiang, Y.; Neyshabur, B.; Mobahi, H.; Krishnan, D.; and Bengio, S. 2019. Fantastic generalization measures and where to find them. *arXiv preprint arXiv:1912.02178*.
- Kairouz, P.; McMahan, H. B.; Avent, B.; Bellet, A.; Bennis, M.; Bhagoji, A. N.; Bonawitz, K.; Charles, Z.; Cormode, G.; Cummings, R.; et al. 2019. Advances and open problems in federated learning. *arXiv preprint arXiv:1912.04977*.
- Karimireddy, S. P.; Kale, S.; Mohri, M.; Reddi, S.; Stich, S.; and Suresh, A. T. 2020. SCAFFOLD: Stochastic controlled averaging for federated learning. In *International Conference on Machine Learning*, 5132–5143. PMLR.
- Keskar, N. S.; Mudigere, D.; Nocedal, J.; Smelyanskiy, M.; and Tang, P. T. P. 2016. On large-batch training for deep learning: Generalization gap and sharp minima. *arXiv preprint arXiv:1609.04836*.
- Kim, M.; Li, D.; Hu, S. X.; and Hospedales, T. 2022. Fisher SAM: Information Geometry and Sharpness Aware Minimization. In *International Conference on Machine Learning*, 11148–11161. PMLR.
- Konečný, J.; McMahan, H. B.; Ramage, D.; and Richtárik, P. 2016a. Federated optimization: Distributed machine learning for on-device intelligence. *arXiv preprint arXiv:1610.02527*.
- Konečný, J.; McMahan, H. B.; Yu, F. X.; Richtárik, P.; Suresh, A. T.; and Bacon, D. 2016b. Federated learning: Strategies for improving communication efficiency. *arXiv preprint arXiv:1610.05492*.
- Krizhevsky, A.; Nair, V.; and Hinton, G. 2009. Cifar-10 and cifar-100 datasets. URL: <https://www.cs.toronto.edu/kriz/cifar.html>, 6.
- Kwon, J.; Kim, J.; Park, H.; and Choi, I. K. 2021. Asam: Adaptive sharpness-aware minimization for scale-invariant learning of deep neural networks. In *International Conference on Machine Learning*, 5905–5914. PMLR.
- Lee, G.; Shin, Y.; Jeong, M.; and Yun, S.-Y. 2021. Preservation of the global knowledge by not-true self knowledge distillation in federated learning. *arXiv preprint arXiv:2106.03097*.
- Lee, S. H.; Lee, S.; and Song, B. C. 2021. Vision transformer for small-size datasets. *arXiv preprint arXiv:2112.13492*.
- Li, H.; Xu, Z.; Taylor, G.; Studer, C.; and Goldstein, T. 2018. Visualizing the loss landscape of neural nets. *Advances in neural information processing systems*, 31.
- Li, Q.; He, B.; and Song, D. 2021. Model-Contrastive Federated Learning. In *Proceedings of the IEEE/CVF Conference on Computer Vision and Pattern Recognition*, 10713–10722.
- Li, T.; Sahu, A. K.; Talwalkar, A.; and Smith, V. 2020a. Federated learning: Challenges, methods, and future directions. *IEEE Signal Processing Magazine*, 37(3): 50–60.

- Li, T.; Sahu, A. K.; Zaheer, M.; Sanjabi, M.; Talwalkar, A.; and Smith, V. 2020b. Federated optimization in heterogeneous networks. *Proceedings of Machine Learning and Systems*, 2: 429–450.
- Li, X.; Huang, K.; Yang, W.; Wang, S.; and Zhang, Z. 2019. On the convergence of fedavg on non-iid data. *arXiv preprint arXiv:1907.02189*.
- Luo, M.; Chen, F.; Hu, D.; Zhang, Y.; Liang, J.; and Feng, J. 2021. No Fear of Heterogeneity: Classifier Calibration for Federated Learning with Non-IID Data. *arXiv preprint arXiv:2106.05001*.
- Marfoq, O.; Neglia, G.; Vidal, R.; and Kamani, L. 2022. Personalized federated learning through local memorization. In *International Conference on Machine Learning*, 15070–15092. PMLR.
- McMahan, B.; Moore, E.; Ramage, D.; Hampson, S.; and y Arcas, B. A. 2017. Communication-efficient learning of deep networks from decentralized data. In *Artificial Intelligence and Statistics*, 1273–1282. PMLR.
- Mendieta, M.; Yang, T.; Wang, P.; Lee, M.; Ding, Z.; and Chen, C. 2022. Local Learning Matters: Rethinking Data Heterogeneity in Federated Learning. In *Proceedings of the IEEE/CVF Conference on Computer Vision and Pattern Recognition*, 8397–8406.
- Mi, P.; Shen, L.; Ren, T.; Zhou, Y.; Sun, X.; Ji, R.; and Tao, D. 2022. Make sharpness-aware minimization stronger: A sparsified perturbation approach. *arXiv preprint arXiv:2210.05177*.
- Nesterov, Y. E. 1983. A method for solving the convex programming problem with convergence rate $O(1/k^2)$. In *Dokl. akad. nauk Sssr*, volume 269, 543–547.
- Netzer, Y.; Wang, T.; Coates, A.; Bissacco, A.; Wu, B.; and Ng, A. Y. 2011. Reading digits in natural images with unsupervised feature learning. *NIPS Workshop on Deep Learning and Unsupervised Feature Learning 2011*.
- Oh, J.; Kim, S.; and Yun, S.-Y. 2021. Fedbabu: Towards enhanced representation for federated image classification. *arXiv preprint arXiv:2106.06042*.
- Oord, A. v. d.; Li, Y.; and Vinyals, O. 2018. Representation learning with contrastive predictive coding. *arXiv preprint arXiv:1807.03748*.
- Paszke, A.; Gross, S.; Massa, F.; Lerer, A.; Bradbury, J.; Chanan, G.; Killeen, T.; Lin, Z.; Gimelshein, N.; Antiga, L.; Desmaison, A.; Kopf, A.; Yang, E.; DeVito, Z.; Raison, M.; Tejani, A.; Chilamkurthy, S.; Steiner, B.; Fang, L.; Bai, J.; and Chintala, S. 2019. PyTorch: An Imperative Style, High-Performance Deep Learning Library. In Wallach, H.; Larochelle, H.; Beygelzimer, A.; d'Alché-Buc, F.; Fox, E.; and Garnett, R., eds., *Advances in Neural Information Processing Systems 32*, 8024–8035. Curran Associates, Inc.
- Qu, Z.; Li, X.; Duan, R.; Liu, Y.; Tang, B.; and Lu, Z. 2022. Generalized Federated Learning via Sharpness Aware Minimization. *arXiv preprint arXiv:2206.02618*.
- Simonyan, K.; and Zisserman, A. 2014. Very deep convolutional networks for large-scale image recognition. *arXiv preprint arXiv:1409.1556*.
- Stich, S. U. 2018. Local SGD converges fast and communicates little. *arXiv preprint arXiv:1805.09767*.
- Sun, Y.; Shen, L.; Chen, S.; Ding, L.; and Tao, D. 2023a. Dynamic Regularized Sharpness Aware Minimization in Federated Learning: Approaching Global Consistency and Smooth Landscape. *arXiv preprint arXiv:2305.11584*.
- Sun, Y.; Shen, L.; Huang, T.; Ding, L.; and Tao, D. 2023b. FedSpeed: Larger local interval, less communication round, and higher generalization accuracy. *arXiv preprint arXiv:2302.10429*.
- Torralba, A.; Fergus, R.; and Freeman, W. T. 2008. 80 million tiny images: A large data set for nonparametric object and scene recognition. *IEEE transactions on pattern analysis and machine intelligence*, 30(11): 1958–1970.
- Wang, H.; Yurochkin, M.; Sun, Y.; Papailiopoulos, D.; and Khazaeni, Y. 2020a. Federated learning with matched averaging. *arXiv preprint arXiv:2002.06440*.
- Wang, J.; Liu, Q.; Liang, H.; Joshi, G.; and Poor, H. V. 2020b. Tackling the objective inconsistency problem in heterogeneous federated optimization. *arXiv preprint arXiv:2007.07481*.
- Wang, P.; Zhang, Z.; Lei, Z.; and Zhang, L. 2023. Sharpness-aware gradient matching for domain generalization. In *Proceedings of the IEEE/CVF Conference on Computer Vision and Pattern Recognition*, 3769–3778.
- Woodworth, B.; Patel, K. K.; Stich, S.; Dai, Z.; Bullins, B.; McMahan, B.; Shamir, O.; and Srebro, N. 2020. Is local SGD better than minibatch SGD? In *International Conference on Machine Learning*, 10334–10343. PMLR.
- Yang, J.; Shi, R.; Wei, D.; Liu, Z.; Zhao, L.; Ke, B.; Pfister, H.; and Ni, B. 2023. MedMNIST v2-A large-scale lightweight benchmark for 2D and 3D biomedical image classification. *Scientific Data*, 10(1): 41.
- Yang, Q.; Liu, Y.; Chen, T.; and Tong, Y. 2019. Federated machine learning: Concept and applications. *ACM Transactions on Intelligent Systems and Technology (TIST)*, 10(2): 1–19.
- Zhang, L.; Shen, L.; Ding, L.; Tao, D.; and Duan, L.-Y. 2022. Fine-tuning global model via data-free knowledge distillation for non-iid federated learning. In *Proceedings of the IEEE/CVF Conference on Computer Vision and Pattern Recognition*, 10174–10183.
- Zhao, Y.; Li, M.; Lai, L.; Suda, N.; Civin, D.; and Chandra, V. 2018. Federated learning with non-iid data. *arXiv preprint arXiv:1806.00582*.
- Zhuang, J.; Gong, B.; Yuan, L.; Cui, Y.; Adam, H.; Dvornik, N.; Tatikonda, S.; Duncan, J.; and Liu, T. 2022. Surrogate gap minimization improves sharpness-aware training. *arXiv preprint arXiv:2203.08065*.

A Table of Notations

Table 5: Table of Notations throughout the paper.

Indices:	
k	Index for clients ($k \in [K]$)
g	Index for global server
Environment:	
\mathcal{D}	Whole dataset
\mathcal{D}^k	Local dataset of the k -th client
α	Parameter for the Dirichlet Distribution
s	The number of shards per user
FL algorithms:	
β, μ	Multiplicative coefficient for the proximal loss
γ	Learning rate
τ	Temperature of probability distribution
ρ	Perturbation Radius for SAM-related algorithms
Λ	Vector consists with scaling parameters for perturbation vector in SAM-related algorithms
Weights:	
w_g	Weight of the global server model on the round t
w_k	Weight of the k -th client model on the round t
$\ w_g - w_k\ $	Collection of L^2 -norm between server and client models, among all rounds.
Objective Functions:	
$\mathcal{L}_{\text{local}}^k$	Local objective for the k -th client
\mathcal{L}_p^k	Proximal Loss for the k -th client

B Experimental Setups

The code is implemented by PyTorch (Paszke et al. 2019). The overall code structure is based on FedML (He et al. 2020) library with some modifications for simplicity. We use 2 A6000 GPU cards, but without Multi-GPU training.

B.1 Model Architecture

For the primary experiments, we use the model architecture used in FedAvg (McMahan et al. 2017), which consists of two convolutional layers with subsequent max-pooling layers, and two fully-connected layers. The same model is also used in (Lee et al. 2021; Li, He, and Song 2021; Luo et al. 2021). We also conduct experiments on ResNet-18 (He et al. 2016), Vgg-11 (Simonyan and Zisserman 2014), and SL-ViT (Lee, Lee, and Song 2021). For SL-ViT, we resize

28×28 -sized images into 32×32 to fit in the required minimum patch size.

B.2 Datasets

To validate our algorithm, we employ 6 distinct datasets, as listed below. The values in the parentheses denote the number of samples used to *train* and *test*, respectively.

- **MNIST** (Deng 2012) (60,000 / 10,000): contains handwritten digits images, ranging from 0 to 9. The data is augmented using Random Cropping, Random Horizontal Flipping, and Normalization. The data is converted to 3-channel RGB images.
- **CIFAR-10** (Krizhevsky, Nair, and Hinton 2009) (50,000 / 10,000): contains a labeled subset of 80 Million Tiny Images (Torralba, Fergus, and Freeman 2008) for 10 different classes. The data is augmented using Random Cropping, Horizontal Flipping, Normalization, and Cutout (DeVries and Taylor 2017).
- **SVHN** (Netzer et al. 2011) (73,257 / 26,032): contains digits of house numbers obtained from *Google Street View*. The data is augmented using Random Cropping, Random Horizontal Flipping, and Normalization.
- **CINIC-10** (Darlow et al. 2018) (90,000 / 90,000): contains a combination of CIFAR and downsized ImageNet (Deng et al. 2009), which is compiled to serve as a bridge between the two datasets. The data is augmented using Random Cropping, Random Horizontal Flipping, and Normalization.
- **PathMNIST** (Yang et al. 2023) (110,000 / 7,180): contains non-overlapping patches from Hematoxylin & Eosin stained colorectal cancer histology slide images. The data is augmented using Random Horizontal Flipping, and Normalization.
- **TissueMNIST** (Yang et al. 2023) (189,106 / 47,280): contains microscope images of human kidney cortex cells, which are segmented from 3 reference tissue specimens. The data is augmented using Random Horizontal Flipping, and Normalization. The data is converted to 3-channel RGB images.

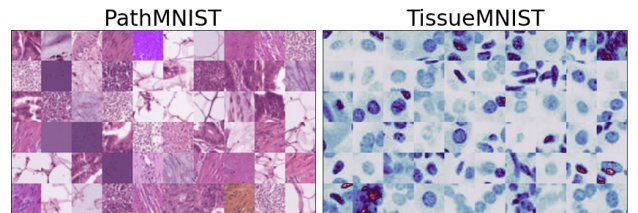


Figure 9: Example images from PathMNIST datasets and TissueMNIST datasets.

Note that we evaluate our algorithm is on medical imaging datasets - a crucial practical application of federated learning (Aledhari et al. 2020; Yang et al. 2019). Illustrative examples of the images are in Figure 9.

B.3 Non-IID Partition Strategy

To comprehensively address the data heterogeneity issue in federated learning, we distribute the local datasets using the following two distinct data partition strategies: (i) **Sharding** and (ii) **Latent Dirichlet Allocation (LDA)**.

- **(i) Sharding** (McMahan et al. 2017; Oh, Kim, and Yun 2021; Lee et al. 2021): sorts the data by label and divide the data into shards of the same size, and distribute them to the clients. In this strategy, the heterogeneity level increases as the shard per user, s , becomes smaller, and vice versa. As the number of shards is the same across all the clients, *the dataset size is identical for each client*.
- **(ii) Latent Dirichlet Allocation (LDA)** (Luo et al. 2021; Wang et al. 2020a; Li, He, and Song 2021): allocates the data samples of class c to each client k with the probability p_c , where $p_c \approx \text{Dir}(\alpha)$. In this strategy, *both the distribution and dataset size differ for each client*. The heterogeneity level increases as the concentration parameter, α , becomes smaller, and vice versa.

Note that although only the statistical distributions varies across the clients in Sharding strategy, both the distribution and dataset size differ in LDA strategy.

B.4 Learning Setups

We use a momentum SGD optimizer with an initial learning rate of 0.01, a momentum value of 0.9, and weight decay $1e-5$. The momentum is employed only for local learning and is not uploaded to the server. Note that SAM optimization also requires its base optimizer, which performs the parameter update using the obtained gradient at the perturbed weights. The learning rate is decays with a factor of 0.99. As we are assuming a synchronized FL scenario, we simulate the parallel distributed learning by sequentially conducting local learning for the sampled clients and then aggregate them into a global model. The standard deviation is measured over 3 runs. The detailed learning setups for each datasets is provided in Table 6.

Table 6: Learning scenarios for each datasets.

Datasets	Clients	Comm. Rounds	Sampling Ratio
MNIST	100	200	0.1
CIFAR-10	100	300	0.1
SVHN	100	200	0.1
CINIC-10	200	300	0.05
PathMNIST	200	200	0.05
TissueMNIST	200	200	0.05

B.5 Algorithm Implementation Details

We search for hyperparameters and select the best among the candidates. The hyperparameters for each method is provided in Table 7. In the primary experiments, we use KL-divergence loss (Hinton, Vinyals, and Dean 2015) with softened logits with temperature $\tau=3$ for the proximal loss for the weight perturbation in FedSoL.

Table 7: Algorithm-specific hyperparameters.

Methods	Selected	Searched Candidates
FedAvg	None	None
FedProx	$\mu=1.0$	$\mu \in \{0.1, 0.5, 1.0, 2.0\}$
Scaffold	None	None
FedNova	None	None
FedNTD	$\beta=1.0, \tau=1.0$	$\beta \in \{0.5, 1.0\}, \tau \in \{1.0, 3.0\}$
FedSAM	$\rho=0.1$	$\rho \in \{0.1, 0.5, 1.0, 2.0\}$
FedASAM	$\rho=1.0$	$\rho \in \{0.1, 0.5, 1.0, 2.0\}$
FedDyn	None	None
MOON	$\mu=0.1, \tau=0.5$	$\mu \in \{0.1, 0.5\}, \tau \in \{0.5, 1.0\}$
FedSoL	$\rho = 2.0$	$\rho \in \{0.1, 0.5, 1.0, 2.0\}$

C Learning Curves

To provide further insights into the learning process, we illustrate the learning curves of different FL methods in Figure 10. Although we utilize different communication rounds for each dataset, the performance of the model becomes sufficiently saturated at the end of communication rounds. For all datasets, FedSoL not only achieves a superior final model at the end of the communication round but also demonstrates much faster convergence. Moreover, although some algorithms that perform well on a dataset fail on another (ex. FedNTD (Lee et al. 2021) underperforms compared to FedProx (Li et al. 2020b) on the TissueMNIST datasets), FedSoL consistently exhibits significant improvements when compared to the other baselines.

D Personalized Performance

In Table 8, we compare FedSoL with several methods specifically designed for personalized federated learning (pFL): PerFedAvg (Fallah, Mokhtari, and Ozdaglar 2020), FedBabu (Oh, Kim, and Yun 2021), and kNN-Per (Marfoq et al. 2022). Each method is assessed by fine-tuning them for e local epochs from the global model after the final communication round. As global alignment is unnecessary for the personalized model, we fine-tune FedSoL using original the local objective without perturbation and denote it as FedSoL-FT. The standard deviation is measured across the clients. The results reveal that our FedSoL-FT consistently outperforms other pFL methods under various scenarios. Furthermore, the gap is enlarged when local ($e=1$), implying that the global model obtained by FedSoL adapts more quickly to local distributions. We suggest that by integrating FedSoL with other methods specialized for pFL, we can attain superior performance for both the global server model and client local models.

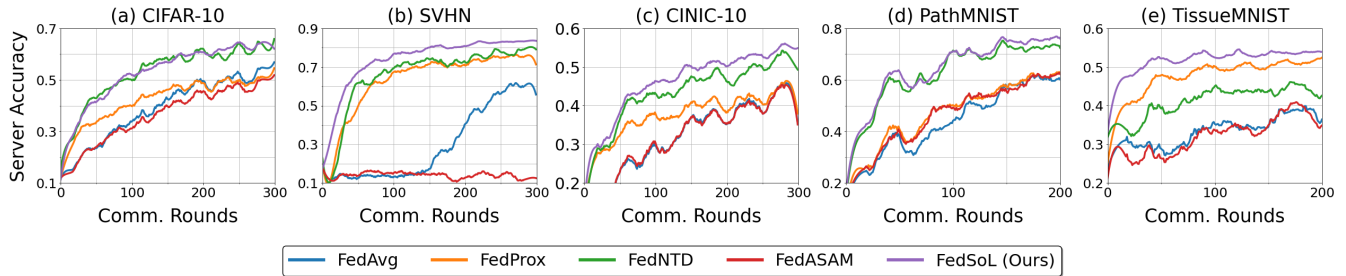


Figure 10: Learning curves of FL methods on LDA ($\alpha=0.1$). The curves are smoothed for clear visualization.

Table 8: Personalized FL performance after τ epochs of fine-tuning. The heterogeneity level is set as LDA ($\alpha = 0.1$).

Method	e	CIFAR-10	SVHN	TissueMNIST
Local-only	-	84.7 \pm 12.8	87.4 \pm 13.0	82.4 \pm 15.5
FedAvg	1	84.1 \pm 13.4	86.6 \pm 15.5	82.2 \pm 17.5
	5	88.9 \pm 8.9	92.1 \pm 5.7	89.2 \pm 10.1
PerFedAvg	1	80.5 \pm 16.2	64.1 \pm 30.3	82.3 \pm 18.9
	5	86.3 \pm 10.4	72.4 \pm 21.2	88.8 \pm 10.2
FedBabu	1	84.6 \pm 12.7	88.7 \pm 9.6	85.7 \pm 14.3
	5	89.2 \pm 8.4	92.7 \pm 6.2	90.5 \pm 8.8
kNN-Per	1	85.7 \pm 12.3	86.4 \pm 15.0	86.5 \pm 14.2
	5	89.7 \pm 8.1	92.8 \pm 6.2	91.4 \pm 7.5
FedSoL-FT (Ours)	1	87.5 \pm 9.7	92.5 \pm 7.4	88.1 \pm 12.2
	5	90.5 \pm 7.8	95.0 \pm 3.9	91.6 \pm 6.9

E Proximal Perturbation with SAM

In our work, we consider how to combine the proximal restriction into SAM optimization to improve overall FL performance. A straightforward approach might involve using the linearly combined local objective between the original local loss $\mathcal{L}_{\text{local}}^k$ and the proximal loss \mathcal{L}_p^k in Equation (2) for the SAM optimization in Equation (3) as follows:

$$\min_{\mathbf{w}_k} \max_{\|\epsilon\|_2 < \rho} [\mathcal{L}_{\text{local}}^k(\mathbf{w}_k) + \beta \cdot \mathcal{L}_p^k(\mathbf{w}_k; \mathbf{w}_g)]. \quad (12)$$

In the above equation, the gradients for weight perturbation and parameter update are obtained from the same objective.

However, this approach encounters the same drawbacks as when using each method on its own. The combined loss also varies considerably across clients due to heterogeneous local distributions, causing the smoothness to largely rely on individual local distributions. Furthermore, the negative correlation between the gradients of the two objectives within the combined loss still limits local learning. Consequently, this approach neither encourages global alignment nor preserves the local generality as desired.

Instead in FedSoL, we overcome this issue by decoupling this directly combined loss into the proximal loss \mathcal{L}_p^k for weight perturbation and the original local loss $\mathcal{L}_{\text{local}}^k$ for weight updates. To further analyze the relationship between

loss functions and weight perturbation in SAM optimization, we conduct an ablation study on the following strategies.

- A_0 : Use original local loss without any weight perturbation (**FedAvg**).
- A_1 : Use original local loss, but get the original local loss gradient at weights perturbed by the proximal gradient (**FedSoL**).
- A_2 : Use combined loss, but get the proximal loss gradient at weights perturbed by the proximal gradient.
- A_3 : Use combined loss, but get the proximal loss gradient at weights perturbed by the proximal gradient.
- A_4 : Use combined loss, but get the combined loss gradient at weights perturbed by the combined gradient.
- A_5 : Use combined loss without any weight perturbation (**Proximal Restriction**).
- A_6 : Use combined loss, but get the original local loss gradient at proximally perturbed weight loss.

We exclude the strategies that obtaining proximal loss at the perturbed weights using the original local loss gradient i.e., $\mathcal{L}_p(\mathbf{w}_k + \epsilon_c^*)$, where $\epsilon_c^* = \rho \frac{\mathbf{g}_p + \mathbf{g}_l}{\|\mathbf{g}_p + \mathbf{g}_l\|}$, as it leads the learning to diverge. The detailed formulation for each method is provided in Table 9 with its corresponding performance. The results in Table 9 demonstrates that utilizing the original local loss gradient at weights perturbed by the proximal loss gradient (A_1 in Table 9) yields outperforms the other approaches. We suggest that our FedSoL is an effective way to integrate proximal restriction effect into SAM optimization in FL.

Table 9: Detailed formulation for each method and their performance on CIFAR-10 datasets (LDA $\alpha=0.1$).

Name	Method Formulation	Performance
A_0	$\mathcal{L}_{\text{local}}(\mathbf{w}_k)$	56.13
A_1	$\mathcal{L}_{\text{local}}(\mathbf{w}_k + \epsilon_p^*)$	64.13
A_2	$\mathcal{L}_{\text{local}}(\mathbf{w}_k) + \beta \cdot \mathcal{L}_p(\mathbf{w}_k + \epsilon_p^*)$	53.85
A_3	$\mathcal{L}_{\text{local}}(\mathbf{w}_k + \epsilon_p^*) + \beta \cdot \mathcal{L}_p(\mathbf{w}_k + \epsilon_p^*)$	60.28
A_4	$\mathcal{L}_{\text{local}}(\mathbf{w}_k + \epsilon_c^*) + \beta \cdot \mathcal{L}_p(\mathbf{w}_k + \epsilon_c^*)$	45.72
A_5	$\mathcal{L}_{\text{local}}(\mathbf{w}_k) + \mathcal{L}_p(\mathbf{w}_k)$	61.76
A_6	$\mathcal{L}_{\text{local}}(\mathbf{w}_k + \epsilon_p^*) + \beta \cdot \mathcal{L}_p(\mathbf{w}_k)$	44.12

F Proof of Proposition

We begin by organizing Equation (7), substituting Equation (6) into FedSoL:

$$\begin{aligned}\Delta^{\text{FedSoL}} \mathcal{L}_{\{\text{local}, p\}}^k(\mathbf{w}_k) &\approx -\gamma \langle \nabla_{\mathbf{w}_k} \mathcal{L}_{\{\text{local}, p\}}^k(\mathbf{w}_k), \mathbf{g}_u(\mathbf{w}_k) \rangle \\ &\approx -\gamma \left(\langle \nabla_{\mathbf{w}_k} \mathcal{L}_{\{\text{local}, p\}}^k(\mathbf{w}_k), \mathbf{g}_l \rangle + \rho \langle \nabla_{\mathbf{w}_k} \mathcal{L}_{\{\text{local}, p\}}^k(\mathbf{w}_k), \nabla^2 \mathcal{L}_{\text{local}}^k \hat{\mathbf{g}}_p \rangle \right),\end{aligned}\quad (13)$$

and for the update of $\mathcal{L}_{\text{local}}^k(\mathbf{w}_k)$ in FedAvg:

$$\Delta^{\text{FedAvg}} \mathcal{L}_{\text{local}}^k(\mathbf{w}_k) \approx -\gamma \langle \nabla_{\mathbf{w}_k} \mathcal{L}^k(\mathbf{w}_k), \mathbf{g}_l \rangle = -\gamma \|\nabla \mathcal{L}_{\text{local}}^k(\mathbf{w}_k)\|^2. \quad (14)$$

E.1 Proof of Proposition 1

Regarding Proposition 1, from Equation (13), we obtain:

$$\Delta^{\text{FedSoL}} \mathcal{L}_p^k \approx -\gamma \left(\langle \mathbf{g}_p, \mathbf{g}_l \rangle + \rho \langle \mathbf{g}_p, \nabla^2 \mathcal{L}_{\text{local}}^k \hat{\mathbf{g}}_p \rangle \right) \approx -\gamma \left(\langle \mathbf{g}_l, \mathbf{g}_p \rangle + \rho \cdot \hat{\mathbf{g}}_p^\top \nabla^2 \mathcal{L}_{\text{local}}^k \mathbf{g}_p \right).$$

Furthermore, if the local objective is convex, then the Hessian is always positive semi-definite. Consequently, $\mathbf{g}_p^\top \nabla^2 \mathcal{L}_{\text{local}}^k \mathbf{g}_p \geq 0$, and we can guarantee that the second term is nonnegative as well.

E.2 Proof of Proposition 2

Similarly, from Equation (13), we derive:

$$\begin{aligned}\Delta^{\text{FedSoL}} \mathcal{L}_{\text{local}}^k(\mathbf{w}_k) &\approx -\gamma \left(\langle \nabla_{\mathbf{w}_k} \mathcal{L}_{\text{local}}^k(\mathbf{w}_k), \nabla_{\mathbf{w}_k} \mathcal{L}_{\text{local}}^k(\mathbf{w}_k) \rangle + \rho \langle \nabla_{\mathbf{w}_k} \mathcal{L}_{\text{local}}^k(\mathbf{w}_k), \nabla_{\mathbf{w}_k}^2 \mathcal{L}_{\text{local}}^k \hat{\mathbf{g}}_p \rangle \right) \\ &= -\gamma \left(\|\nabla_{\mathbf{w}_k} \mathcal{L}_{\text{local}}^k(\mathbf{w}_k)\|^2 + \frac{\rho}{2} \langle \hat{\mathbf{g}}_p, 2\nabla_{\mathbf{w}_k}^2 \mathcal{L}_{\text{local}}^k \nabla_{\mathbf{w}_k} \mathcal{L}_{\text{local}}^k(\mathbf{w}_k) \rangle \right) \\ &= -\gamma \left(\|\nabla_{\mathbf{w}_k} \mathcal{L}_{\text{local}}^k(\mathbf{w}_k)\|^2 + \nabla_{\mathbf{w}_k} \|\nabla_{\mathbf{w}_k} \mathcal{L}_{\text{local}}^k(\mathbf{w}_k)\|^2 \cdot \frac{\rho}{2} \hat{\mathbf{g}}_p \right).\end{aligned}$$

On the other hand, from Equation (14), applying the first-order Taylor approximation to $\mathbf{w}_k \mapsto \|\nabla \mathcal{L}_{\text{local}}^k(\mathbf{w}_k)\|^2$, we have:

$$\begin{aligned}\Delta^{\text{FedAvg}} \mathcal{L}_{\text{local}}^k \left(\mathbf{w}_k + \frac{\rho}{2} \hat{\mathbf{g}}_p \right) &\approx -\gamma \|\nabla_{\mathbf{w}_k} \mathcal{L}_{\text{local}}^k \left(\mathbf{w}_k + \frac{\rho}{2} \hat{\mathbf{g}}_p \right)\|^2 \\ &\approx \gamma \left(\|\nabla_{\mathbf{w}_k} \mathcal{L}_{\text{local}}^k(\mathbf{w}_k)\|^2 + \nabla_{\mathbf{w}_k} \|\nabla_{\mathbf{w}_k} \mathcal{L}_{\text{local}}^k(\mathbf{w}_k)\|^2 \cdot \frac{\rho}{2} \hat{\mathbf{g}}_p \right).\end{aligned}$$

Therefore, $\Delta^{\text{FedAvg}} \mathcal{L}_{\text{local}}^k \left(\mathbf{w}_k + \frac{\rho}{2} \hat{\mathbf{g}}_p \right)$ is equal to $\Delta^{\text{FedSoL}} \mathcal{L}_{\text{local}}^k(\mathbf{w}_k)$, up to the first-order Taylor approximation.